Available online at www.worldscientificnews.com

World Scientific News

An International Scientific Journal

WSN 191 (2024) 168-188 EISSN 2392-2192

Mathematical Model Investigating the Impact of Pharmaceutical and Non-Pharmaceutical Approaches on the Spread and Control of COVID-19 in Uganda

Nuwamanya Dasan[1], **Onuorah Martins Onyekwelu**[2,*] and **Mohammed Abdullahi Baba**[1]

[1] Department of Mathematics & Statistics, School of Mathematics and Computing, Kampala International University, Main Campus, Kampala, Uganda

[2] Department of Computer Science, School Science, and Technology, Kigali Independent University, Kigali, Rwanda

*E-mail address: monuorah2015@gmail.com

ABSTRACT

In this paper, a model that incorporates pharmaceutical and non-pharmaceutical interventions for asymptotic and symptomatic COVID-19 was developed and analyzed qualitatively and quantitatively. The basic reproduction number R_0, was obtained using the next-generation matrix approach, and the parameters that drive the infection were identified through the sensitivity analysis of the R_0. To determine the model's short- and long-term behavior, the disease-free and endemic equilibrium states were obtained and analyzed for stability or otherwise. The model was validated using the cumulative number of confirmed COVID-19 cases in Uganda from March 21 to July 21, 2020. In line with the paper's aim, we simulated the effects of pharmaceutical and non-pharmaceutical intervention measures on targeted epidemiological compartments.

***Keywords*:** COVID-19, Stability, Equilibrium, Basic reproduction number, Simulation

(Received 16 February 2024; Accepted 11 March 2024; Date of Publication 13 March 2024)

1. INTRODUCTION

Origin of COVID-19

The COVID-19 pandemic's SARS-CoV-2 virus, which is currently ravaging the world, has been actively affecting people before January 2020, when its pathogenic potential detonated in full force in Wuhan. It's believed that SARS-COV-2 was responsible for the emergence of small disease outbreaks in Wuhan, a province in China, and most likely elsewhere that did not reach epidemic proportions. The general genesis may be tracked back to environmental changes that have reduced animals' natural habitats, considerably enabling animals to come closer to humans and pathogen-carrying animal reservoirs, including SARS-CoV-2 which causes COVID-19 (Platto et al., 2021). The genesis of SARS-CoV-2 is a hotly disputed topic, with both natural and laboratory unintentional leak ideas gaining traction. The latter encompasses two excluding hypotheses: the accidental release of a biological virus or the accidental release of a virus. COVID-19- began on December 8, 2019, at the seafood market called Huanan Seafood Wholesale Market (HSWM) in Wuhan (Frutos et al., 2022). Based on a phylogenetic study (Foster et al., 2021) coronavirus was baptized as a severe acute respiratory syndrome coronavirus 2 abbreviated as (SARS-CoV-2) by the International Committee on Taxonomy of Viruses that is responsible for naming these occurring viruses. SARS-CoV-2 is believed to have emanated from a virus that formally infected animals and evolved into a highly contagious virus. Most people all around the globe are currently infected with coronavirus disease 2019 (COVID-19), and it is the fifth pandemic ever recorded after the 1918 influenza pandemic (Liu et al., 2020). According to the results of several AI-enabled tests utilizing clustering algorithms, bats or pangolins may have been the virus's first host (Nguyen et al., 2020).

Reports show that the African continent was the last to be hit by the COVID-19 epidemic and the least afflicted. Africa recorded 19,895 confirmed cases from 52 nations as of April 18, 2020, with a fatality rate of 5.1 percent. Egypt confirmed her first case on February 14, 2020, followed chronologically by a West African country called Algeria, which reported its very first case on February 25, and Nigeria on February 27. Apart from these three countries, the first instances in other African countries were only confirmed in early March of 2021, with Uganda reporting its first case on March 21, 2020. (Lone & Ahmad, 2020). Uganda reported 157,160 cumulative cases as of January 12, 2022, with 98,859 cumulative recoveries, 178 ongoing cases admitted to health facilities around the country, and 3,385 cumulative COVID-19-associated deaths. (MoH UG, 2022)

Going through the literature, we cite the following studies of COVID-19 with pharmaceutical interventions. (Choi et al., 2021) created an age-structured model to explain COVID-19 transmission dynamics, including immunization. They calculated the risk of infection for individual age categories in Korea in various levels of social distance and locked down. (Foy et al., 2021) extensively worked on a mathematical model to compare COVID-19 vaccine distribution tactics in India. They assessed age-specific vaccine allocation strategies in India using an age structure and an enhanced SEIR model with a mass action contact matrix.

(Anggriani et al., 2022) developed, examined, and validated a COVID-19 mathematical model. The asymptomatic and symptomatic compartments, as well as reduced immunity, were considered in the model. (Sharma et al., 2021) established a meditative fuzzy correlation technique for patients of COVID-19 from various locations in India based on the criteria. The proposed mediative fuzzy correlation technique found a link between COVID-19-positive patients' increments and the passage of time. (Ali et al., 2021) presented a technology to help

health practitioners with prioritizing and scheduling COVID-19 patient's challenges, based on Artificial Intelligence (AI) and Operations Research (OR) using a Fuzzy Interval. The findings showed that reducing the models produced a practical assessment under limited baseline data to pick an acceptable patient list for a set of institutions.

The proposed method enabled the achievement of a significant goal: lowering death rates within each hospital's resource limits. (Gad et al., 2021) described the dynamics of COVID-19 using a new fractional-order mathematical model. They separated the population into eight classes in the proposed model, with three epidemiological categories utilized to evaluate parameters with their initial values.

For COVID-19 models with non-pharmaceutical interventions, we cite the following; (Mugisha et al., 2021), formulated a deterministic ODE model to ascertain the transmission dynamics of COVID-19 disease in Uganda and the implications of complacency plus easing the lockdown early. Their findings showed that even if Uganda gets rid of all imported cases, it will take close to nine months to eliminate the disease from the population. (Sameni, 2020), looked at how social factors, including distance, regional lockdowns, quarantine, and worldwide public health alertness, influenced model parameters to reflect the dynamic behavior of outbreaks on a regional basis. (Engbert et al., 2021) introduced sequential data assimilation to the stochastic SEIR epidemic model. (Senapati et al., 2021), proposed a mathematical model to characterize the disease transmission process between persons in India and evaluate the impact of preventative measures on the number of new cases. To capture illness progression, (Adak et al., 2021) used a deterministic model with four compartments encompassing the health epidemiological status of a population. Further, the deterministic model was extended to the stochastic model to account for the uncertainty or variance in illness transmissibility. (Abdullahi et al., 2021) created a mathematical model to evaluate the lockdown in Nigeria. The analysis of their model includes stability, computing of equilibrium, determination of the basic reproductive proportion, and transient stability of the equilibrium points. (Sitthiwirattham et al., 2021) discussed a discrete form of the SEIR model and explained the principal propagation of COVID-19 and control for the rapid development of this viral disease in real life. (Yang & Wang, 2021); included both human-to-human and human-to-environment transmission paths and various transmission rates to depict epidemiological characteristics across time. (Kouidere et al., 2021) described the dynamics of the COVID-19 transmission by using Pontryagin's maximum theorem to analyze some of the optimal controls and an iterative technique to solve the optimality system.

(Ahmad et al., 2021) created a mathematical model that included the resistive and quarantine classes and applied it to the transmission dynamics of the novel coronavirus disease (COVID-19) that appeared only once. (Atangana et al., 2021) constructed models for coronavirus disease at various stages, adding new parameters due to individual interactions. They investigated several critical computational simulations and sensitivity assessments. By using two singular kernel fractional derivative operators, (Singh et al., 2021) investigated the dynamics of the SEIR compartmental model. They used this strategy to analyze the model's entire memory effects. (Shahzad et al., 2021) constructed models for coronavirus disease at various stages, adding new parameters due to individual interactions. They looked into several critical computational simulations and sensitivity assessments.

(Zamir et al., 2021) used a non-clinical strategy to investigate the best way to control the emerging COVID-19 pandemic. They also used a sensitivity test to determine the sensitivity indices of the parameters involved in disease transmission and to identify the most

active/sensitive parameters for analyzing the propagation of COVID-19. Using event data from West Java Province, Indonesia. (Singh et al., 2021), aiming to determine how lockdown affects the new coronavirus (COVID-19) dynamics. The dynamics of a COVID-19 stochastic model with an isolation strategy were examined by (Danane et al., 2021). The proposed model included white noise and L'evy jump perturbations. (Muller & Muller, 2021) created a model to assess and analyze the effectiveness of various containment tactics, such as house-to-house testing, surveillance testing of people, contact tracing, and self-control measures like mask-wearing and social distancing. The rest of the paper is organized as follows; in section 2, the model's logic is presented, followed by the schematic diagram, model parameters, and the positivity of the model solution. Section 3 was devoted to the equilibrium states, their stability analysis, the basic reproduction number, its contour plot, and the sensitivity analysis. In section 4, the model fitted to real data and thereafter simulated to ascertain the effects of the pharmaceutical and non-pharmaceutical interventions. While in section 5 contains the conclusion, recommendation, and further research.

2. FORMULATION OF THE MODEL

In formulating the model, we represent the total population at time t by $(N(t))$ and subdivide it into; Susceptible $(S(t))$, Exposed $(E(t))$, Quarantined $(Q(t))$, Asymptomatically Infected $(I_A(t))$, Symptomatically Infected $(I_S(t))$, Hospitalized $(H(t))$, and Recovered $(R(t))$

Hence, $N(t) = S(t) + E(t) + Q(t) + I_A(t) + I_s(t) + H(t) + R(t)$ (1)

The susceptible population is increased via the recruitment of infected immigrants into the populations at a constant rate Λ. They are reduced once the susceptible population interacts with the infected population and gets exposed at the rate of κ and hence the mass action is given by κIS. The susceptible population dies naturally at the rate of δ. The exposed compartment is comprised of the susceptible population that gets into contact with those infected with COVID-19. This class is reduced by those who are quarantined, those who progress to the infected class after testing positive during the incubation period, and those who die naturally. Quarantine class, a non-pharmaceutical control measure, comprises those who get exposed and then quarantined, as well as immigrants who are quarantined at the point of entry. This class is reduced by those who test negative and return to the susceptible class, those who test positive and are hospitalized, and those who die naturally from this class. This class comprises people who test positive for COVID-19 but are not showing any symptoms, although they can transmit the disease to their contacts.

This class is drained by those who recover without being hospitalized, those who are hospitalized, and those who die naturally. This class is comprised of people who test positive for COVID-19 and are visibly showing the signs and symptoms. The class is reduced by those hospitalized and those who die naturally from this class. The class consists of the people who test positive and are drawn from the quarantined, asymptotically infected, and symptomatically infected classes. The class is drained by those who die of COVID-19-related infection and those who die naturally, as well as those who recover from the COVID-19 infection. This class is filled with the population from the asymptomatically infected class who recover without getting

hospitalized and those who recover from the infection from the hospitalized class. The class is drained by those who lose immunity and go back to the susceptible class as well as those who die naturally from this class.

The diagram below demonstrates how COVID-19 disease moves from one epidemiological compartment to another.

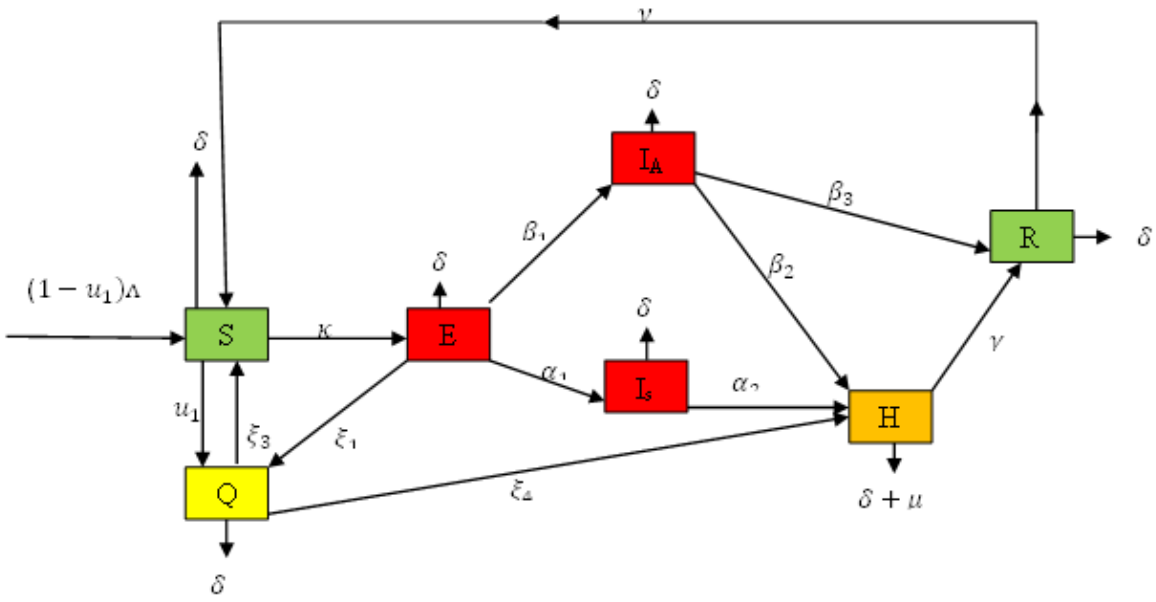

Figure 1. The schematic diagram of the model

2. 1. The Model equations

Following the model formulation and the schematic diagram in Figure 1 above, we present the model as follows:

$$\left.\begin{aligned}
\frac{dS}{dt} &= (1-u_1)\Lambda - (\kappa(\eta I_A + I_s)u_2 - \delta)S + \nu R + \xi_3 Q \\
\frac{dE}{dt} &= \kappa u_2 S(\eta I_A + I_s) - (\delta + \xi_1 + \alpha_1 + \beta_1)E \\
\frac{dQ}{dt} &= u_1\Lambda + \xi_1 E - (\xi_3 + \xi_4 + \delta)Q \\
\frac{dI_A}{dt} &= \beta_1 E - (\beta_2 + \delta + \beta_3)I_A \\
\frac{dI_s}{dt} &= \alpha_1 E - (\alpha_2 + \delta)I_s \\
\frac{dH}{dt} &= u_2\Lambda + \beta_2 I_A + \alpha_2 I_s + \xi_4 Q - (\delta + \gamma + \mu)H \\
\frac{dR}{dt} &= \gamma H + \beta_3 I_A - (\nu + \delta)R
\end{aligned}\right\} \qquad (2)$$

With initial conditions

$$S(0) = S_0, E(0) = E_0, Q(0) = Q_0, I(0) = I_0, H(0) = H_0, R(0) = R_0 = 0.$$

Table 1. Table showing the state variables and parameters of the model.

State Variable		**Description**	
S		Susceptible class	
E		Exposed class	
Q		Quarantined class	
I_A		Asymptomatically infected class	
I_s		symptomatically infected class	
H		Hospitalized class	
R		Recovered class	
Parameter	**Value**		**Source**
Λ	0.023 per day	Recruitment rate	(Anggriani et al., 2022)
δ	0.006838 per annum	Natural death rate	(UBOS, 2019)
κ	0.002 per day	The rate at which the susceptible get exposed.	(Yavuz et al., 2021)
ξ_1	0.45 per day	The rate at which the exposed are quarantined	Assumed
ξ_3	0.4 per day	The rate at which the quarantined return to susceptible	(Liang, 2020)
ξ_4	0.8 per week	The rate at which the quarantined are hospitalized.	(Ngonghala et al., 2020)
β_1	0.5944 per day	The rate at which the exposed become asymptomatically infected.	(Mcintosh, 2020)
β_2	0.2 per day	The rate at which the asymptomatically infected are hospitalized	(Colizzi et al., 2020)
β_3	0.962 per day	The rate at which the asymptomatically infected	Calibrated

		recover without getting hospitalized.	
α_1	0.8 per day	The rate at which exposed become symptomatically infected	(Mcintosh, 2020)
α_2	0.9	The rate at which the symptomatically infected are hospitalized	Calibrated
γ	0.8	The rate at which the hospitalized recover from COVID-19 infection.	(Ngonghala et al., 2020)
μ	0.02197 per day	COVID-19 related death	(Ngonghala et al., 2020)
u_1	0.81 per day	The proportion of tested immigrants	Calibrated
u_2	0.0012	The proportion of people who practice social distancing	Assumed
ν	0.998 per day	The rate at which the recovered class returns to the susceptible class	Assumed

2. 2. Positivity of the solution of the model

Lemma 1

Let $\Re_+^7 = \left\{N[t] \in \Re_+^7 : N[t] \geq 0\right\};\ N(t) = \left[S(t), E(t), Q(t), I_A(t) I_s(t), H(t), R(t)\right]^T$ (3)

The solution set N(t) of the considered system of the ODE for the model with respect to the stated initial conditions must be non-negative for all t > 0 in $\Re_+^7$ (Yavuz et al., 2021)

From the first equation of (2)

$$\frac{dS}{dt} = -(\kappa(\eta I_A + I_s)u_2 - \delta)S$$

Separating variables,

$$\int \frac{dS}{S} \geq -\int (\kappa(\eta I_A + I_s)u_2 + \delta)dt\ ;\ \ln S \geq -(\kappa(I_A + I_s)u_2 + \delta)t\ ;\ S \geq e^{-(\kappa(I_A+I_s)u_{22}+\delta)t} \quad (4)$$

$$S(t) \geq S(0)e^{-(\kappa(\eta I_A+I_s)u_2+\delta)t}\ ;\ S(t) \geq 0$$

Repeating the same for the other compartments, we have.

$$S(t), E(t), Q(t), I_A(t), I_s(t), H(t), R(t) \geq 0 \forall t > 0 \quad (5)$$

Hence the solution can't escape the hyperplane $S = E = Q = I_A = I_s = H = R = 0$. Furthermore, the vector field on each hyperplane falls into implying that the feasible region is a positive constant.

3. EQUILIBRIUM STATES OF THE MODEL

3. 1. Disease-free equilibrium of the model

The disease-free equilibrium (DFE) of the model is given by

$$(S^*, E^*, Q^*, I_A^*, I_S^*, H^*, R^*) = \left(\frac{(1-u_1)\Lambda}{\delta}, 0, 0, 0, 0, 0, 0 \right) \quad (6)$$

3. 2. Endemic equilibrium of the model

The endemic equilibrium of the model is given by equations (7) to 13).

$$S^{**} = \frac{-(k_5 k_4 k_6 k_7 k_8 k \wedge k_3) - (k_4 k_2 \kappa l \beta_1 k_6 k_7 k_8 \wedge)}{((l((-k_7 k_8 k_3 k_4 + \xi_1(v\gamma\xi_4 + k_7 k_8 \xi_3))\, k_5 + \beta_1 k_4 v(\gamma\beta_2 + k_7 \beta_3))\kappa k_2 + k_5(k_4 \delta k_8 k_7 + (v\gamma\xi_4 + k_7 k_8 \xi_3))k_3)k_6 + v k_4 k_2 \kappa l \alpha_2 k_5 \alpha_1 \gamma)}, \quad (7)$$

$$E^{**} = \frac{-(k_5 k_4 k_2 k l k_6 k_7 k_8 k \wedge)}{(((l(-k_7 k_8 k_3 k_4 + \xi_1(v\gamma\xi_4 + k_7 k_8 \xi_3))\kappa k_2 + (-k_4 \delta k_8 k_7 + (v\gamma\xi_4 + k_7 k_8 \xi_3))k_3)k_5 + l v \kappa k_2 k_4 \beta_1(\gamma\beta_2 + k_7 \beta_3))k_6 + v k_4 k_2 \kappa l \alpha_2 k_5 \alpha_2 \gamma)}, \quad (8)$$

$$Q^{**} = \frac{-(k_5(l\kappa k_2 \xi_1 + k_3)k_6 k_7 k_8 k \wedge)}{(((l(-k_7 k_8 k_3 k_4 + \xi_1(v\gamma\xi_4 + k_7 k_8 \xi_3))\kappa k_2 + (-k_4 \delta k_8 k_7 + (v\gamma\xi_4 + k_7 k_8 \xi_3))k_3)k_5 + l v \kappa k_2 k_4 \beta_1(\gamma\beta_2 + k_7 \beta_3))k_6 + v k_4 k_2 \kappa l \alpha_2 k_5 \alpha_1 \gamma)}, \quad (9)$$

$$I_A^{**} = \frac{-(k_4 k_2 \kappa l \beta_1 k_6 k_7 k_8 \wedge)}{((l((-k_7 k_8 k_3 k_4 + \xi_1(v\gamma\xi_4 + k_7 k_8 \xi_3))\, k_5 + \beta_1 k_4 v(\gamma\beta_2 + k_7 \beta_3))\kappa k_2 + k_5(k_4 \delta k_8 k_7 + \xi_2(v\gamma\xi_4 + k_7 k_8 \xi_3))k_3)k_6 + v k_4 k_2 \kappa l \alpha_2 k_5 \alpha_1 \gamma}, \quad (10)$$

$$I_S^* = \frac{-k_4 k_2 \kappa l \alpha_2 k_5 \alpha_1 \gamma) \wedge)}{((l((+k_7 k_8 k_3 k_4 + \xi_1(v\gamma\xi_4 + k_7 k_8 \xi_3))\, \kappa k_2 + (-k_4 \delta k_8 k_7 + \xi_2(v\gamma\xi_4 + k_7 k_8 \xi_3))k_3)\, k_6 + v k_4 k_2 \kappa l \alpha_2 k_5 \alpha_1 \gamma)k_5 + l v \kappa k_2 k_4 \beta_1(\gamma\beta_2 + k_7 \beta_3))}, \quad (11)$$

$$H^{**} = \frac{-(k((\xi_4((l\kappa k_2 \xi_1 + k_3)k_5 + k_4 k_2 \kappa l \beta_1 \beta_2)k_6 + k_4 k_2 \kappa l \alpha_2 k_5 \alpha_1)k_8 \wedge)}{(((l(-k_7 k_8 k_3 k_4 + \xi_1(v\gamma\xi_4 + k_7 k_8 \xi_3))\kappa k_2 + (-k_4 \delta k_8 k_7 + \xi_2(v\gamma\xi_4 + k_7 k_8 \xi_3))k_3)k_5 + l v \kappa k_2 k_4 \beta_1(\gamma\beta_2 + k_7 \beta_3))k_6 + v k_4 k_2 \kappa l \alpha_2 k_5 \alpha_1 \gamma)}, \quad (12)$$

$$R^{**} = \frac{-(k(((k_4\xi_4\,\gamma\xi_1 + k_4\beta_1(\gamma\beta_4 + k_7\beta_3))l\,\kappa\,k_2 + k_5\xi_4\,\gamma\,k_3)k_6 + k_4k_2\,\kappa\,l\,\alpha_2k_5\,\alpha_1\,\gamma)\wedge)}{((l((+k_7k_8k_3k_4 + \xi_1(\nu\gamma\xi_4 + k_7k_8\xi_3))\,k_5 + \beta_1\,k_4\nu(\gamma\beta_2 + k_7\,\beta_3))\kappa k_2 + k_5(k_4\,\delta k_8k_7 + \xi_2\,(\nu\gamma\xi_4 + k_7k_8\xi_3))k_3)k_6 + \nu\,k_4k_2\,\kappa\,l\,\alpha_2k_5\alpha_1\,\gamma)} \quad (13)$$

where: $k_1 = 1-u_1, k_2 = (\kappa(I_A + I_s)u_2 - \delta)$, $k_3 = \delta + \xi_1 + \alpha_1 + \beta_1$, $k_4 = \xi_3 + \xi_4 + \delta$ $k_5 = \beta_2 + \delta + \beta_3$, $k_6 = \alpha_2 + \delta$, $k_7 = \delta + \gamma + \mu$, $k_8 = \nu + \delta$.

3. 3. Basic reproductive number of the model

The basic Reproduction number is the total number of secondary infections resulting from the entrance of an infective individual into a population where everybody is susceptible. It's denoted by and is an important threshold that plays a major role in public health policy aimed at disease control. It is also known that when $R_0 < 1$ the disease-free equilibrium is stable. Considering infective classes, and applying the next-generation matrix method, we have that the F and V of our model are

$$F := \begin{bmatrix} 0 & 0 & \frac{u_2ku_1\wedge}{\delta} & \frac{u_2ku_1\wedge}{\delta} & 0 \\ 0 & 0 & 0 & 0 & 0 \\ 0 & 0 & 0 & 0 & 0 \\ 0 & 0 & 0 & 0 & 0 \\ 0 & 0 & 0 & 0 & 0 \end{bmatrix} \quad (14)$$

$$V := \begin{bmatrix} k_3 & 0 & 0 & 0 & 0 \\ -\zeta_1 & k_4 & 0 & 0 & 0 \\ -\beta_1 & 0 & k_5 & 0 & 0 \\ -\alpha_1 & 0 & 0 & k_6 & 0 \\ 0 & -\zeta_4 & -\beta_2 & -\alpha_2 & k_7 \end{bmatrix} \quad (15)$$

$$FV^{-1} = \begin{bmatrix} \frac{u_2ku_1\wedge\beta_1}{\delta k_3k_5} + \frac{u_2ku_1\wedge\alpha_1}{\delta k_3k_6} & 0 & \frac{u_2ku_1\wedge}{\delta k_5} & \frac{u_2ku_1\wedge}{\delta k_6} & 0 \\ 0 & 0 & 0 & 0 & 0 \\ 0 & 0 & 0 & 0 & 0 \\ 0 & 0 & 0 & 0 & 0 \\ 0 & 0 & 0 & 0 & 0 \end{bmatrix} \quad (16)$$

Using the characteristic equation; $FV - \lambda I = 0$

$$FV^{-1}-\lambda I=\begin{bmatrix} \frac{u_2 k u_1 \wedge \beta_1}{\delta k_3 k_5}+\frac{u_2 k u_1 \wedge \alpha_1}{\delta k_3 k_5}-\lambda & 0 & \frac{u_2 k u_1 \wedge}{\delta k_5} & \frac{u_2 k u_1 \wedge}{\delta k_6} & 0 \\ 0 & -\lambda & 0 & 0 & 0 \\ 0 & 0 & -\lambda & 0 & 0 \\ 0 & 0 & 0 & -\lambda & 0 \\ 0 & 0 & 0 & 0 & -\lambda \end{bmatrix}=0 \quad (17)$$

$$\left[[\lambda_1=0],[\lambda=0],[\lambda_2=0],[\lambda_3=0],\left[\lambda_4=\frac{k\wedge u_2 u_1\left(k_5\alpha_1+k_6\beta_1\right)}{\delta k_3 k_5 k_6}\right]\right] \quad (18)$$

$$R_0=\frac{k\wedge u_2 u_1\left(k_5\alpha_1+k_6\beta_1\right)}{\delta k_3 k_5 k_6}. \quad (19)$$

3. 4. Sensitivity analysis of the basic reproduction number

The word "sensitivity index" is frequently used to describe the sensitivity analysis of a variable quantity about model parameters, quantifying the relative change in the variable quantity whenever a model parameter changes. The normalized forward sensitivity index, table 2, was computed using;

$$\Gamma_{\varpi}^{R_0}=\frac{\partial R_0}{\partial \varpi}\times\frac{\varpi}{R_0}$$

where ϖ represents the parameters of the basic reproduction number of the model are presented in Table 2. The sensitivity analysis of the model basic reproductive number (Table 2) shows that the three most sensitive parameters are u_2, Λ and κ followed by α_2, while the least sensitive is δ followed by β_2.

Table 2. Sensitivity indices of the parameters of R_0 .

Parameter	Sensitive Value
Λ	1
δ	-0.0119
κ	1
α_1	0.4601
α_2	0.9924
β_1	-0.0718
β_2	-0.0184
β_3	-0,0887

u_1	-0.4594
u_2	1
ξ_1	-0.2431

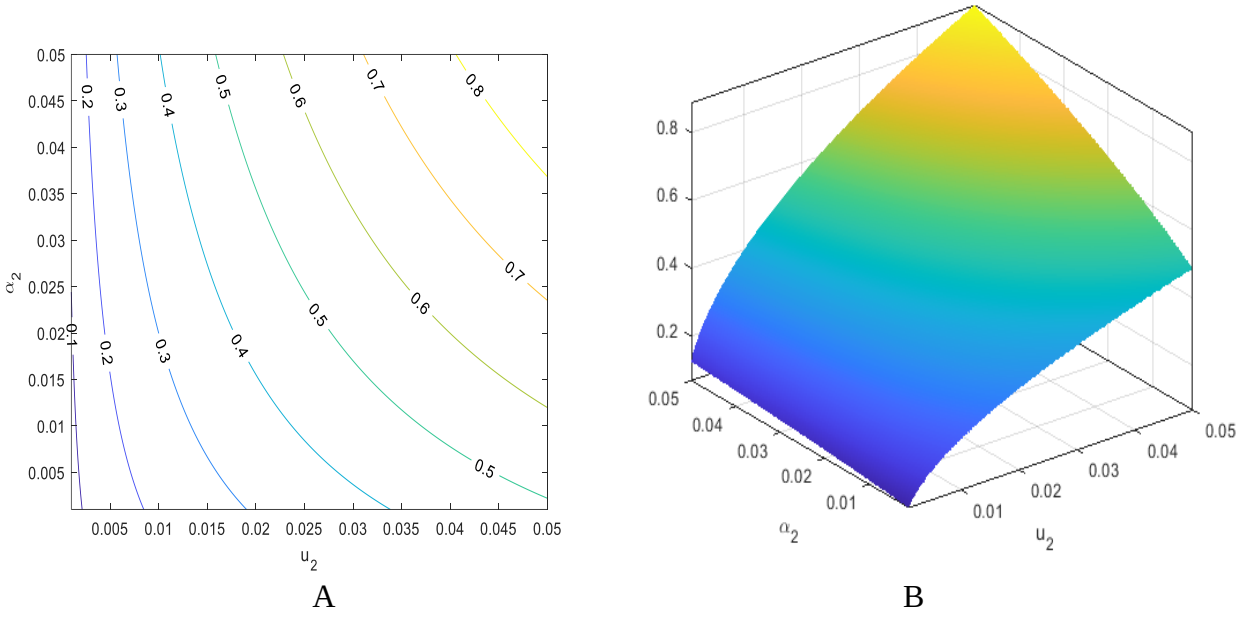

Figure 2. The 2-dimensional **(A)** and 3-dimensional **(B)** contour plot of the basic reproduction number with respect to the hospitalization rate of symptomatically infected (α_2) and the percentage of those that practice social distancing (u_2)

3. 5. Local stability at disease-free equilibrium

Theorem 1

If $R_0 \leq 1$, then DFE is locally asymptotically stable on $\Re_+^7$ hence the local stability on the nonnegative octant heptagon. This means the disease will naturally die from the population. (Diagne et al., 2021)

Proof

To prove the local stability, we use a linearized system for the Jacobean matrix system at DFE using the characteristic equation $A - \lambda I = 0$ where A is the Jacobean.

Differentiating the system (2) with respect to; $(S, E, Q, I_A, I_s, H, R)$ we get the Jacobean as shown in the subsequent matrix

$$A_{DFE}=\begin{bmatrix} -\delta & 0 & \xi_3 & -\frac{u_2\kappa u_1\Lambda}{\delta} & -\frac{u_2\kappa u_1\Lambda}{\delta} & 0 & \nu \\ 0 & -k_3 & 0 & \frac{u_2\kappa u_1\Lambda}{\delta} & \frac{u_2\kappa u_1\Lambda}{\delta} & 0 & 0 \\ 0 & \xi_1 & -k_4 & 0 & 0 & 0 & 0 \\ 0 & \beta_1 & 0 & -k_5 & 0 & 0 & 0 \\ 0 & \alpha_1 & 0 & 0 & -k_6 & 0 & 0 \\ 0 & 0 & \xi_4 & \beta_2 & \alpha_2 & -k_7 & 0 \\ 0 & 0 & 0 & \beta_3 & 0 & \gamma & -k_8 \end{bmatrix} \tag{20}$$

$$A_{DFE}=\begin{bmatrix} -\delta-\lambda & 0 & \xi_3 & -\frac{u_2\kappa u_1\Lambda}{\delta} & -\frac{u_2\kappa u_1\Lambda}{\delta} & 0 & \nu \\ 0 & -k_3-\lambda & 0 & \frac{u_2\kappa u_1\Lambda}{\delta} & \frac{u_2\kappa u_1\Lambda}{\delta} & 0 & 0 \\ 0 & \xi_1 & -k_4-\lambda & 0 & 0 & 0 & 0 \\ 0 & \beta_1 & 0 & -k_5-\lambda & 0 & 0 & 0 \\ 0 & \alpha_1 & 0 & 0 & -k_6-\lambda & 0 & 0 \\ 0 & 0 & \xi_4 & \beta_2 & \alpha_2 & -k_7-\lambda & 0 \\ 0 & 0 & 0 & \beta_3 & 0 & \gamma & -k_8-\lambda \end{bmatrix}=0 \tag{21}$$

Determinant of the Jacobean matrix

$$\begin{aligned} &\frac{1}{\delta}\Big(\big(-\lambda^4+(-\delta-k_7-k_4-k_8)\lambda^3+\big((-k_4-k_7-k_8)\delta+(-k_4-k_8)k_7-k_8k_4 \\ &+\xi_2\xi_3\big)\lambda^2 \quad +\big(\big((-k_4-k_8)k_7-k_8k_4\big)\delta+(-k_4k_8+\xi_2\xi_3)k_7+k_8\xi_2\xi_3\big)\lambda \\ &-k_4k_7k_8\delta+\xi_2\left(v\gamma\xi_4+k_7k_8\xi_3\right)\big) \quad \left(\lambda^3\delta+\delta\left(k_3+k_5+k_6\right)\lambda^2+\big(\big((k_3+k_6\big)k_5\right. \\ &\left.+k_3k_6\big)\delta-\kappa\Lambda u_1u_2\left(\alpha_1+\beta_1\right)=0\right. \end{aligned} \tag{22}$$

Solving the equation (16) all the values of $\lambda_1, \lambda_2, ..., \lambda_n$ must be less than zero then we conclude that the DFE is locally asymptotically stable. Otherwise, it would be unstable.

3. 6. Global stability of the disease-free equilibrium

Theorem 2

The disease-free equilibrium of the deterministic model the model (2) is globally asymptomatically stable iff $R_0<1$ and unstable iff $R_0>1$ (Xing et al., 2020)

Proof

$$\begin{bmatrix} E' \\ I_A' \\ I_s' \end{bmatrix} = (F-V)\begin{pmatrix} E \\ I_A \\ I_s \end{pmatrix}-\begin{pmatrix} \kappa(I_A+I_s)(S^*-S) \\ 0 \\ 0 \end{pmatrix} \tag{23}$$

$S < S* = (1-u_1)\Lambda = \delta S$; $S < S^* = \frac{(1-u_1)\Lambda}{\delta}$ $\forall$ $t > 0$ It follows that; $\begin{pmatrix} E' \\ I_A' \\ I_s' \end{pmatrix} \leq (F-V)\begin{pmatrix} E \\ I_A \\ I_s \end{pmatrix}$

Since the eigenvalues of the matrix $(F-V)$ have negative real parts, then the DFE is stable whenever $R_0 < 1$. So (E, I_A, I_s), $t \to (0,0,0)t$ as $t \to \infty$

By comparison theorem (Foster & Kinzel, 2021) It follows that; (E, I_A, I_s), $t \to (0,0,0)$ and $S \to \frac{(1-u_1)\Lambda}{\delta}$ as $t \to \infty$, then $(S, E, Q, I_A, I_s, H, R)$, $t \to E_0$, $t \to \infty$. So E_0 is globally asymptomatically stable for $R_0 < 1$

3. 7. Model validation

Models that cannot relate well to live data are assumed to be mere academic exercises that may not help solve a real-life problem. The parameter *values need to* be determined before model simulation; this process of determining the values of the parameters of a model is called model *parameterization*. Parameter values can sometimes be found by performing specific experiments or literature searches. In this research, part of our model parameter values are taken from the literature, and few were found by *calibration*, where parameters are estimated by fitting the model to data. The data used for this purpose is the daily cases of COVID-19 in Uganda from March 21 to July 21, 2020 (Figure 3).

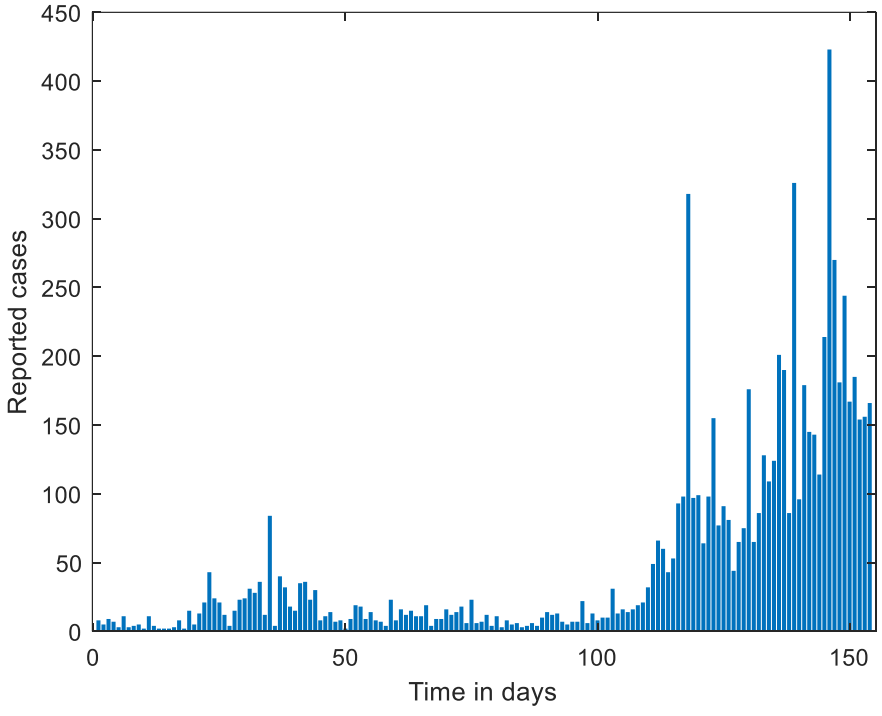

Figure 3. Reported COVID-19 reported cases in Uganda from March 21 to July 21, 2020.

We opted for the least–square approach against interpolation on model validation since the data may contain errors, and capturing every little change in them may be impractical. In the least-squares method, we assume that the time coordinates of the data are exact, but their *y*-coordinates may be distorted. We fit the solution curve through the data in Figure 4 (A) before optimization, and Figure 4 (B) after optimization so that the sum of the squares of the vertical distances from the data points to the point on the curve is as tiny as possible.

In particular, we fitted the cumulative COVID-19 cases $(t_i, Y_i),..., (t_n, Y_n)$, with the sum of squares error $SSE = \sum_{i=1}^{n} (Y_i, E(t_i))^2$. This minimization is implemented using the Matlab function *fminsearch*, the best-fit parameter values from this iterative procedure are then used for model simulation.

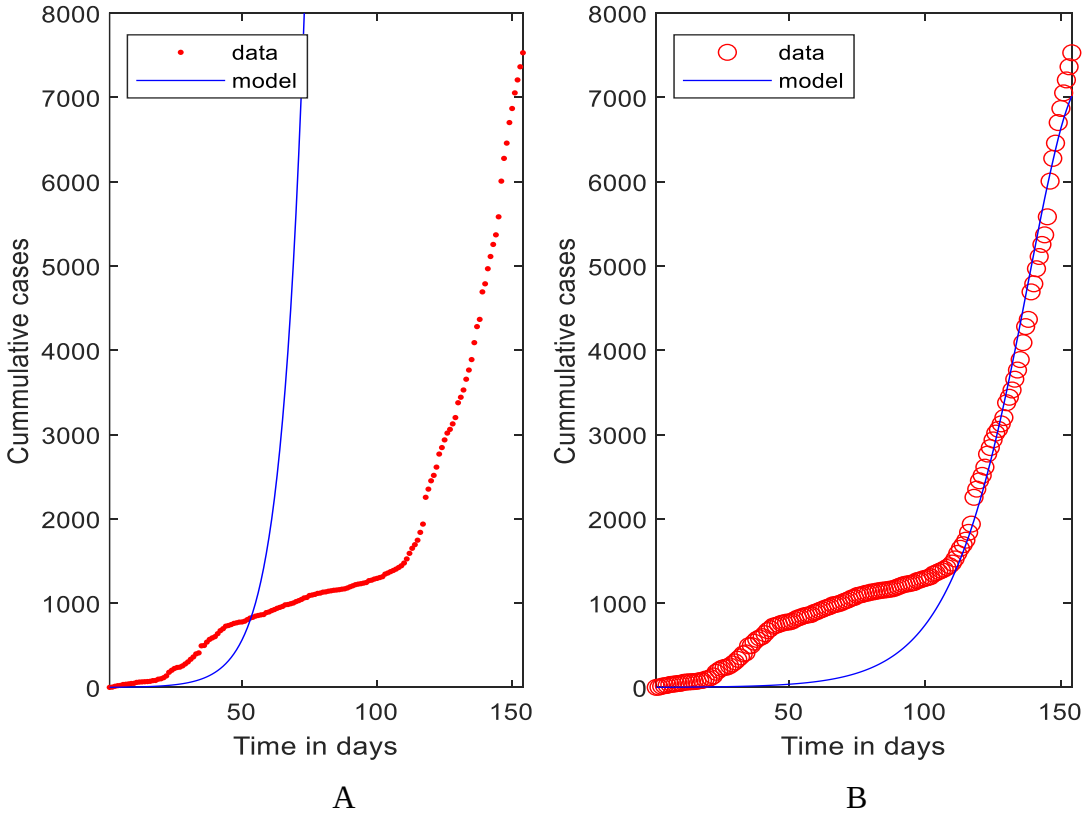

Figure 4. Fitted cumulative COVID-19 data points to the proposed COVID-19 model. Figure 4 **(A)** is before optimization, and figure *(B)* is after optimization.

3. 8. Numerical Simulation

In this section, the simulation of the model was conducted. The graphical relationship of the key pharmaceutical and non-pharmaceutical parameters with respect to the target epidemiological compartments is portrayed. This was achieved using Matlab version R2020a.

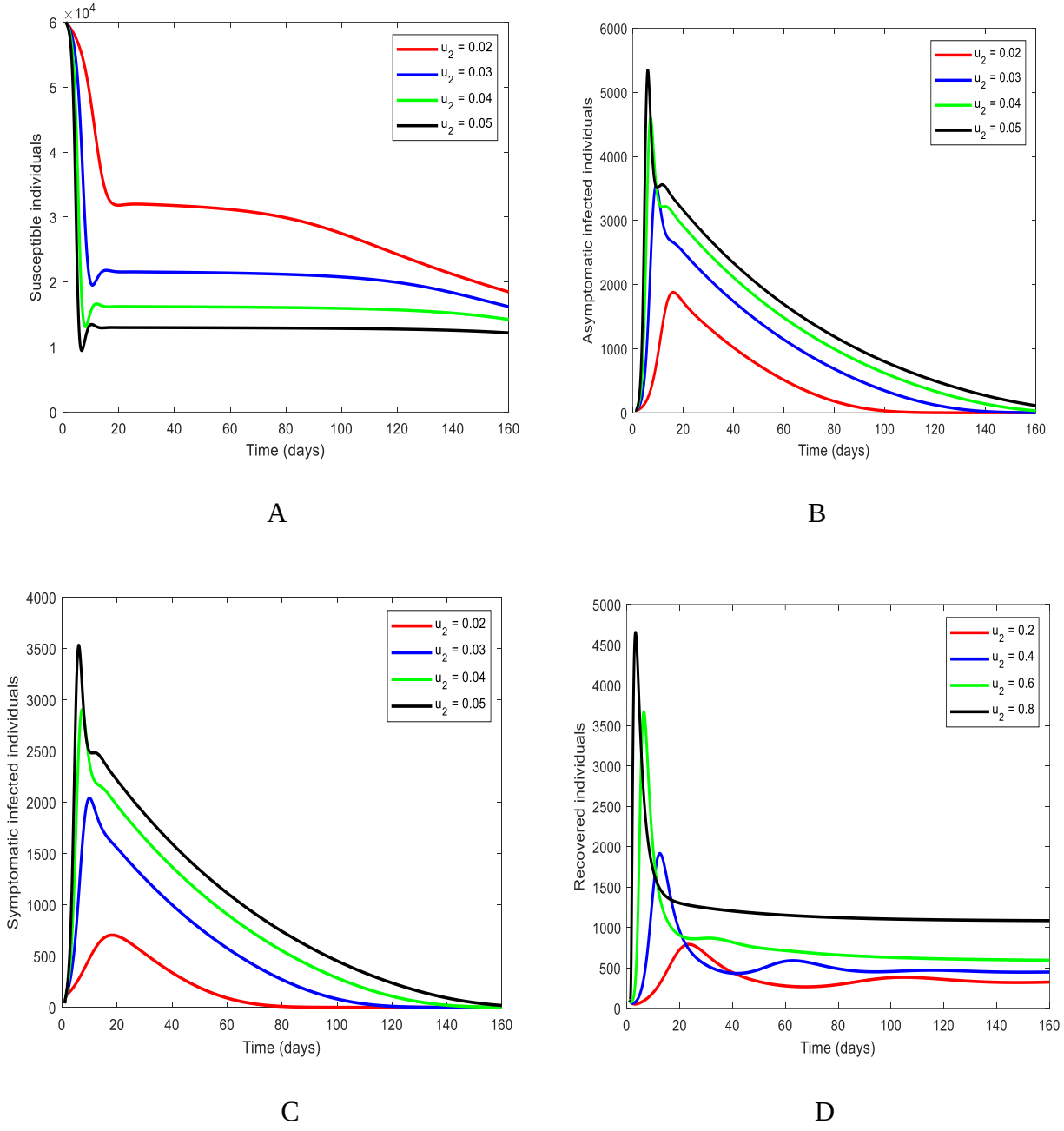

Figure 5. Simulation of susceptible **(A),** asymptomatically infected **(B),** symptomatically infected **(C),** and recovered individuals with respect to the non-pharmaceutical parameter social distance rate, u_2 **(D).**

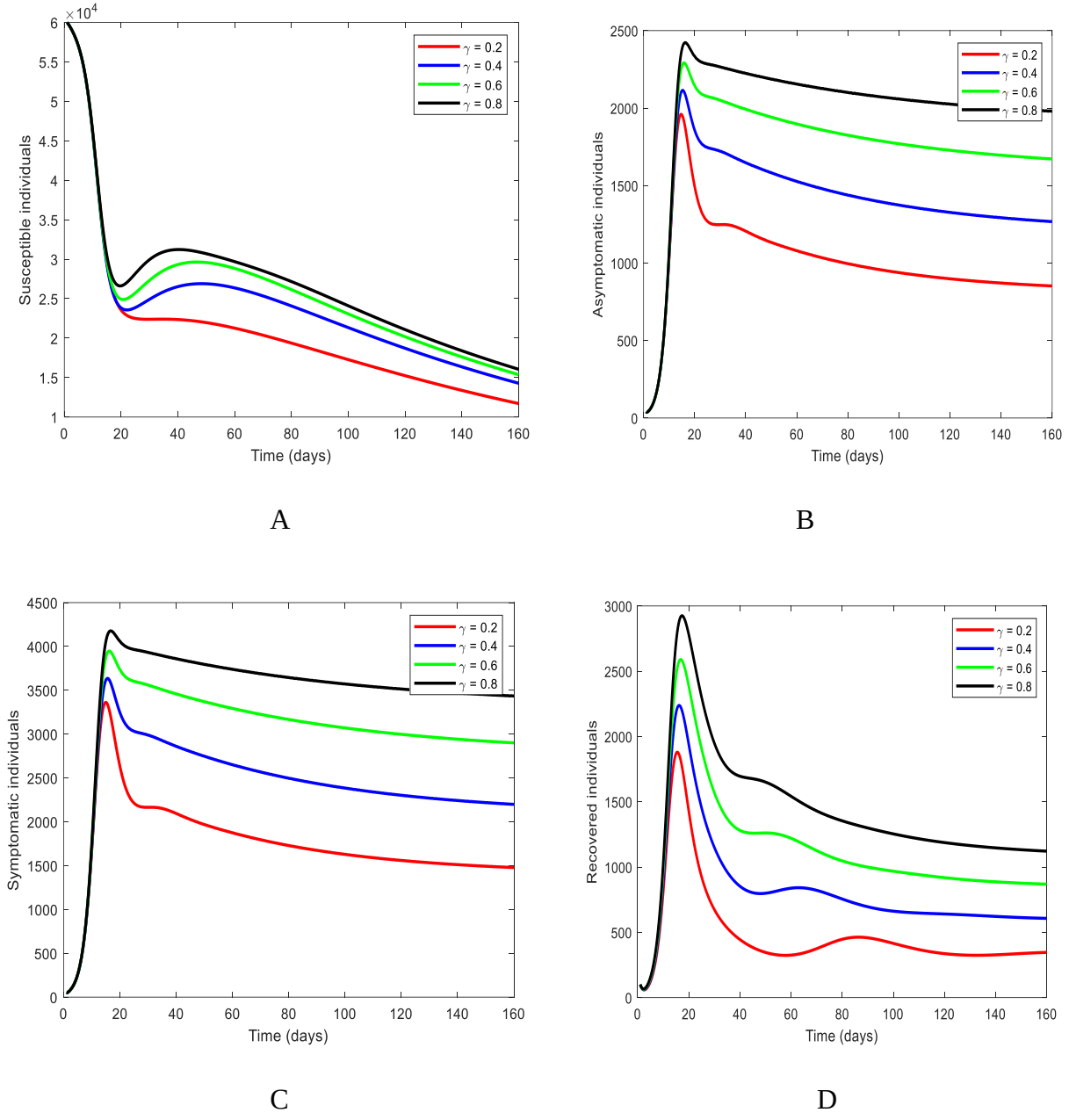

Figure 6. Simulation of susceptible **(A),** asymptomatically infected **(B),** symptomatically infected **(C),** and recovered individuals with respect to the pharmaceutical-induced recovery rate, γ **(D).**

4. SUMMARY AND CONCLUSION

In this paper, a COVID-19 model incorporating pharmaceutical and non-pharmaceutical interventions was studied. The model comprised seven epidemiological compartments; Susceptible (S), Exposed (E), Quarantined (Q), Symptomatically infected (I_s),

Asymptomatically Infected (I_A), Hospitalized (H), and the Recovered (R). The basic properties of the model were also explored, which precedes quantitative analysis. The next-generation matrix was used to compute the basic reproductive number R_O of the model. The model's 2-dimensional and 3-dimensional contour plots The sensitivity analysis of the model basic reproductive number (table 2) shows that the three most sensitive parameters are u_2, Λ and κ followed by α_2, while the least sensitive is δ followed by β_2. Away from the basic reproduction number, the model was validated using the cumulative cases of COVID-19 in Uganda from March 21 to July 21, 2020. Figure 4 (A and B) shows the model validation before and after optimization. The effect of different values of major non-pharmaceutical parameters, and social distancing rate on the susceptible compartment is shown in Figure 5 A, on the asymptomatic compartment, Figure 5 B, symptomatic, Figure 5 C, and recovered, Figure 5 D. The effect of different values of major pharmaceutical parameters, the treatment induced recovery rate on the susceptible compartment is shown on Figure 6 A, on the asymptomatic compartment, Figure 6 B, symptomatic, Figure 6 C, and recovered, Figure 6 D.

Recommendations

The government should strengthen the state of infrastructure such as hospitals and equip them with necessary equipment, such as hospital beds and drugs, to have all those who test positive for COVID-19 hospitalized and treated. Also, testing centers should be extended to every health center II across the country.

Ministry of Health, through local authorities, should ensure that social distancing is encouraged and practiced by all people if they must congregate. At least a distance of two meters apart from one person to another should be adhered to by everyone. This will help to reduce the chances of human-to-human transmission significantly.

Suggestions for Further Studies

The negative impacts of the disease are relatively diverse, as highlighted. Based on this model, it is proposed that researchers can improve the work in the following ways:

- Optimal control model that will determine the most effective control strategies that will minimize the infective compartments.
- Co-infection: This is a great concern in modeling infectious disease, especially since it needs to be investigated and control strategies suggested.
- Climate change: There is a need to investigate the connection between the spread of the disease and climate change and suggest best control strategies.

References

[1] Ahmad, S., Owyed, S., Abdel-Aty, A. H., Mahmoud, E. E., Shah, K., & Alrabaiah, H. (2021). Mathematical analysis of COVID-19 via a new mathematical model. *Chaos, - Solitons & Fractals*, 143, 110585.

[2] Adak, D., Majumder, A., & Bairagi, N. (2021). Chaos, Solitons and Fractals Mathematical perspective of Covid-19 pandemic : Disease extinction criteria in

deterministic and stochastic models. *Chaos, Solitons and Fractals: The Interdisciplinary Journal of Nonlinear Science, and Nonequilibrium and Complex Phenomena*, 142, 110381. https://doi.org/10.1016/j.chaos.2020.110381

[3] Ali, M., Ben, A., & Abdelhedi, M. (2021). Real-time prediction of COVID-19 patient's health situations using Artificial Neural Networks and Fuzzy Interval Mathematical modeling. *Applied Soft Computing*, 110, 107643. https://doi.org/10.1016/j.asoc.2021.107643

[4] Anggriani, N., Ndii, M. Z., Amelia, R., & Suryaningrat, W. (2022). A mathematical COVID-19 model considering asymptomatic and symptomatic classes with waning immunity. *Alexandria Engineering Journal*, 61(1), 113–124. https://doi.org/10.1016/j.aej.2021.04.104

[5] Atangana, A. (2021). A novel COVID-19 model with fractional differential operators with singular and non-singular kernels: Analysis and numerical scheme based on Newton polynomial. *Alexandria Engineering Journal* 60(4), 3781-3806.

[6] Choi, Y., Kim, J. S., Kim, J. E., Choi, H., & Lee, C. H. (2021). Vaccination Prioritization Strategies for COVID-19 in Korea : A Mathematical Modeling Approach. February, 1–19.

[7] Colizzi, M., Bortoletto, R., Silvestri, M., Mondini, F., Puttini, E., Cainelli, C., Gaudino, R., Ruggeri, M., & Zoccante, L. (2020). Brain, Behavior, & Immunity - Health Medically unexplained symptoms in the times of COVID-19 pandemic : A. *Brain, Behavior, & Immunity - Health*, 5(April), 100073. https://doi.org/10.1016/j.bbih.2020.100073

[8] Danane, J., Karam Allali, Zakia Hammouch, Kottakkaran Sooppy Nisar. Mathematical analysis and simulation of a stochastic COVID-19 Lévy jump model with isolation strategy. *Results in Physics*, Volume 23, 2021, 103994, https://doi.org/10.1016/j.rinp.2021.103994

[9] Diagne, M. L., Rwezaura, H., Tchoumi, S. Y., & Tchuenche, J. M. (2021). A Mathematical Model of COVID-19 with Vaccination and Treatment. *Computational and Mathematical Methods in Medicine*, Volume 2021 | Article ID, 1250129https://doi.org/10.1155/2021/1250129

[10] Duhon, J., Bragazzi, N., & Dzevela, J. (2021). Science of the Total Environment The impact of non-pharmaceutical interventions, demographic, social, and climatic factors on the initial growth rate of COVID-19 : A cross-country study. *Science of the Total Environment*, 760, 144325. https://doi.org/10.1016/j.scitotenv.2020.144325

[11] Engbert, R., Rabe, M. M., Reich, S., & Kliegl, R. (2021). Sequential Data Assimilation of the Stochastic SEIR Epidemic Model for Regional COVID-19 Dynamics. *Bulletin of Mathematical Biology*, 83(1), 1–16. https://doi.org/10.1007/s11538-020-00834-8

[12] Foster, A., & Kinzel, M. (2021). Estimating COVID-19 exposure in a classroom setting : A comparison between mathematical and numerical models Estimating COVID-19 exposure in a classroom setting : A comparison between mathematical and numerical models. *Physics of Fluids* 33, 021904, https://doi.org/10.1063/5.0040755

[13] Foy, B. H., Wahl, B., Mehta, K., Shet, A., Menon, G. I., & Britto, C. (2021). International Journal of Infectious Diseases Comparing COVID-19 vaccine allocation strategies in India : A mathematical modeling study. *International Journal of Infectious Diseases*, 103, 431–438. https://doi.org/10.1016/j.ijid.2020.12.075

[14] Frutos, R., Javelle, E., Barberot, C., Gavotte, L., Tissot-dupont, H., & Devaux, C. A. (2022). Origin of COVID-19 : Dismissing the Mojiang mine theory and the laboratory accident narrative. *Environmental Research*, 204(PB), 112141. https://doi.org/10.1016/j.envres.2021.112141

[15] Gad, I., Mohamed, H., Alharthi, M. R., Abdel-aty, A., & Elshehabey, H. M. (2021). Results in Physics Investigation of the dynamics of COVID-19 with a fractional mathematical model : A comparative study with actual data. *Results in Physics*, 23, 103976. https://doi.org/10.1016/j.rinp.2021.103976

[16] Kouidere, A., Kada, D., Balatif, O., Rachik, M., & Naim, M. (2021). Chaos, Solitons, and Fractals Optimal control approach of mathematical modeling with multiple delays of the negative impact of delays in applying preventive precautions against the spread of the COVID-19 pandemic with a case study of Brazil and cost-eff. *Chaos, Solitons and Fractals: The Interdisciplinary Journal of Nonlinear Science, and Nonequilibrium and Complex Phenomena*, 142, 110438. https://doi.org/10.1016/j.chaos.2020.110438

[17] Liu, Y., Kuo, R., & Shih, S. (2020). ScienceDirect COVID-19 : The first documented coronavirus pandemic in history. *Biomedical Journal*, 43(4), 328–333. https://doi.org/10.1016/j.bj.2020.04.007

[18] Lone, S. A., & Ahmad, A. (2020).COVID-19 pandemic – an African perspective, *Emerging Microbes & Infections*, 9:1, 1300-1308, DOI: 10.1080/22221751.2020.1775132

[19] Mcintosh, K. (2020). Coronavirus disease 2019 (COVID-19): Epidemiology, virology, and prevention. *Update*, 1(February), 1–27. https://www.uptodate.com/contents/covid-19-epidemiology-virology-and-prevention

[20] Mugisha JYT, Ssebuliba J, Nakakawa JN, Kikawa CR, Ssematimba A (2021) Mathematical modeling of COVID-19 transmission dynamics in Uganda: Implications of complacency and early easing of lockdown. *PLoS ONE* 16(2): e0247456. https://doi.org/10.1371/journal.pone.0247456

[21] Muller, K., & Muller, P. A. (2021). Mathematical modeling of the spread of COVID-19 on a university campus. *Infectious Disease Modelling*, 6, 1025–1045. https://doi.org/10.1016/j.idm.2021.08.004

[22] Ngonghala, C. N., Iboi, E., Eikenberry, S., Scotch, M., MacIntyre, C. R., Bonds, M. H., & Gumel, A. B. (2020). Mathematical assessment of the impact of non-pharmaceutical interventions on curtailing the 2019 novel Coronavirus. *Mathematical Biosciences*, 325(May), 108364. https://doi.org/10.1016/j.mbs.2020.108364

[23] Thanh Thi Nguyen, Mohamed Abdelrazek, Dung Tien Nguyen, Sunil Aryal, Duc Thanh Nguyen, Sandeep Reddy, Quoc Viet Hung Nguyen, Amin Khatami, Thanh Tam Nguyen, Edbert B. Hsu, Samuel Yang, Origin of novel coronavirus causing COVID-19:

A computational biology study using artificial intelligence, *Machine Learning with Applications,* Volume 9, 2022, 100328, https://doi.org/10.1016/j.mlwa.2022.100328.

[24] Platto, S., Wang, Y., Zhou, J., & Carafoli, E. (2021). Biochemical and Biophysical Research Communications History of the COVID-19 pandemic : Origin, explosion, worldwide spreading. *Biochemical and Biophysical Research Communications*, 538, 14–23. https://doi.org/10.1016/j.bbrc.2020.10.087

[25] Sameni, R. (2020). Mathematical Modeling of Epidemic Diseases; A Case Study of the COVID-19 Coronavirus. *Quantitative Biology* https://doi.org/10.48550/arXiv.2003.11371

[26] Senapati, A., Rana, S., Das, T., & Chattopadhyay, J. (2021). Impact of intervention on the spread of COVID-19 in India : A model-based study. *Journal of Theoretical Biology*, 523, 110711. https://doi.org/10.1016/j.jtbi.2021.110711

[27] Sharma, M. K., Dhiman, N., & Narayan, V. (2021). Mediative fuzzy logic mathematical model : A contradictory management prediction in COVID-19 pandemic. *Applied Soft Computing*, 105, 107285. https://doi.org/10.1016/j.asoc.2021.107285

[28] Singh, A., Pathak, R., & Chaudhary, M. (2021). A SIQ mathematical model on COVID-19 investigating the lockdown effect. *Infectious Disease Modelling*, 6, 244–257. https://doi.org/10.1016/j.idm.2020.12.010

[29] Singh, V., Uduman, P. S. S., & Gómez-aguilar, J. F. (2021). Chaos, Solitons and Fractals Mathematical modeling of coronavirus disease COVID-19 dynamics using CF and ABC non-singular fractional derivatives. *Chaos, Solitons and Fractals: The Interdisciplinary Journal of Nonlinear Science, and Nonequilibrium and Complex Phenomena*, 145, 110757. https://doi.org/10.1016/j.chaos.2021.110757.

[30] Sitthiwirattham, T., Zeb, A., Chasreechai, S., & Eskandari, Z. (2021). Results in Physics Analysis of a discrete mathematical COVID-19 model. *Results in Physics*, 28(July), 104668. https://doi.org/10.1016/j.rinp.2021.104668

[31] UBOS, U. B. of S. (2019). *Uganda Bureau of Statistics the International Labour Day*. 1–19.

[32] Xing, Y., Guo, Z., & Liu, J. (2020). Backward bifurcation in a malaria transmission model. *Journal of Biological Dynamics*, 14(1), 368–388. https://doi.org/10.1080/17513758.2020.1771443

[33] Yang, C., & Wang, J. (2021). Modeling the transmission of COVID-19 in the US e A case study. *Infectious Disease Modelling*, 6, 195–211. https://doi.org/10.1016/j.idm.2020.12.006

[34] Yavuz, M., Coşar, F. Ö., Günay, F., & Özdemir, F. N. (2021). A New Mathematical Modeling of the COVID-19 Pandemic Including the Vaccination Campaign. *Open Journal of Modelling and Simulation*, 09(03), 299–321. https://doi.org/10.4236/ojmsi.2021.93020

[35] Zamir, M., Abdeljawad, T., Nadeem, F., Wahid, A., & Yousef, A. (2021). An optimal control analysis of a COVID-19 model. *Alexandria Engineering Journal*, 60(3), 2875–2884. https://doi.org/10.1016/j.aej.2021.01.022

[36] Zhang, Y. (2021). Non-pharmaceutical interventions during the rollout of COVID-19 vaccines. *BMJ* 2021; 375: n2314. https://doi.org/10.1136/bmj.n2314